LEARNED HARMONIC MEAN ESTIMATION OF THE BAYESIAN EVIDENCE WITH NORMALIZING FLOWS

Alicja Polanska[1]*, Matthew A. Price[1], Davide Piras[2,3], Alessio Spurio Mancini[4,1], and Jason D. McEwen[1,5]†

[1] Mullard Space Science Laboratory, University College London, Dorking, RH5 6NT, UK
[2] Centre Universitaire d'Informatique, Université de Genève, 1227 Genève 4, Switzerland
[3] Département de Physique Théorique, Université de Genève, 24 quai Ernest Ansermet, 1211 Genève 4, Switzerland
[4] Department of Physics, Royal Holloway, University of London, Egham Hill, Egham, UK and
[5] Alan Turing Institute, London, NW1 2DB, UK
Version May 10, 2024

ABSTRACT

We present the learned harmonic mean estimator with normalizing flows – a robust, scalable and flexible estimator of the Bayesian evidence for model comparison. Since the estimator is agnostic to sampling strategy and simply requires posterior samples, it can be applied to compute the evidence using any Markov chain Monte Carlo (MCMC) sampling technique, including saved down MCMC chains, or any variational inference approach. The learned harmonic mean estimator was recently introduced, where machine learning techniques were developed to learn a suitable internal importance sampling target distribution to solve the issue of exploding variance of the original harmonic mean estimator. In this article we present the use of normalizing flows as the internal machine learning technique within the learned harmonic mean estimator. Normalizing flows can be elegantly coupled with the learned harmonic mean to provide an approach that is more robust, flexible and scalable than the machine learning models considered previously. We perform a series of numerical experiments, applying our method to benchmark problems and to a cosmological example in up to 21 dimensions. We find the learned harmonic mean estimator is in agreement with ground truth values and nested sampling estimates. The open-source `harmonic` Python package implementing the learned harmonic mean, now with normalizing flows included, is publicly available. ⬤

1. INTRODUCTION

Model selection plays a crucial role in understanding the complexities of the Universe. It involves the task of identifying the underlying model that best describes observations, for instance of astrophysical phenomena. The field of Bayesian statistics provides a framework for statistical inference and decision-making that incorporates prior knowledge to update probabilities based on observed data. This approach is well-suited for cosmology, for example, as experiments in the field tend to consist of single observations of events, as opposed to repeatable experiments which are at the core of the frequentist framework. As a consequence, Bayesian inference and model comparison are widespread in the field (Trotta 2008). In the Bayesian formalism, an essential tool in this process is the estimation of the Bayesian evidence, also called the marginal likelihood, which quantifies the probability of observed data given a model. The Bayesian evidence allows us to evaluate the relative plausibility of models and assess which hypotheses are best supported by the available data, which is of course not only useful in cosmology but in many other fields.

As a topical illustration of the importance of model selection in cosmology, recent baryon acoustic oscillations measurements from the Dark Energy Spectroscopic

Instrument (DESI Collaboration et al. 2016), combined with observations of the cosmic microwave background (Aghanim et al. 2020; Carron et al. 2022; Madhavacheril et al. 2024) and with supernovae Ia measurements from PantheonPlus (Brout et al. 2022), Union3 (Rubin et al. 2023) or DESY5 (DES Collaboration et al. 2024), provide a tantalizing suggestion of the existence of a time-varying dark energy equation-of-state. Whether dark energy can be described by Einstein's cosmological constant or whether an equation-of-state with $w \neq -1$ is required is a fundamental question of modern cosmology that we hope to answer definitively in the near future through the application of Bayesian model selection techniques to upcoming observational data. We showcase the application of the methodology presented in this article to precisely this question through a simulated Dark Energy Survey (DES) galaxy clustering and weak lensing analysis (cf. Abbott et al. 2018b).

In practice, the computation of Bayesian evidence is very challenging as it involves evaluating a multi-dimensional integral over a potentially highly varied function. The most widespread method for estimating the Bayesian evidence, particularly in astrophysics, is nested sampling (Skilling 2006; Ashton et al. 2022; Buchner 2021). While nested sampling has been highly successful and many effective nested sampling algorithms and codes have been developed (Feroz & Hobson 2008; Feroz et al. 2009a; Feroz et al. 2009b; Brewer et al. 2011;

* E-mail: alicja.polanska.22@ucl.ac.uk
† E-mail: jason.mcewen@ucl.ac.uk

Handley et al. 2015a,b; Feroz et al. 2019; Speagle 2020; Buchner 2021; Williams et al. 2021; Cai et al. 2022), it imposes constraints on the method used to sample. By sampling in a nested manner it is possible to reparameterize the likelihood in terms of the enclosed prior volume such that the evidence can be computed by a one-dimensional integral. The computational challenge then shifts to how to effectively sample in a nested manner, i.e. how to sample from the prior subject to likelihood level-sets or isocontours. The need to sample in this nested manner severely reduces flexibility (hence the need to design custom nested sampling algorithms), typically restricting application to relatively low dimensional settings.[1]

The harmonic mean estimator of the Bayesian evidence, introduced by Newton & Raftery (1994), provides much greater flexibility since it only requires samples from the posterior, available from any Markov chain Monte Carlo (MCMC) method, for example. However, it was immediately realized by Neal (1994) that the method can easily fail catastrophically due to the estimator's variance becoming very large. To solve this issue the learned harmonic mean estimator was recently proposed by McEwen et al. (2021), where machine learning techniques were developed to learn a suitable internal importance sampling target distribution. Since the estimator requires only samples from the posterior and so is agnostic to the method used to generate samples, in contrast to nested sampling, it can be easily applied with any MCMC sampling technique, including saved down MCMC chains, or any variational inference approach. This property also allows the estimator to be adapted to address Bayesian model selection for simulation-based inference (SBI) (Spurio Mancini et al. 2023), where an explicit likelihood is unavailable or infeasible.

In this article we present the use of normalizing flows as the internal machine learning technique within the learned harmonic mean estimator. Normalizing flows can be elegantly coupled with the learned harmonic mean to provide an approach that is more robust, flexible and scalable than the machine learning models considered previously. In Polanska et al. (2023) we presented preliminary work introducing normalizing flow as the machine learning technique within the learned harmonic mean. We fully develop the methodology in the current article, introduce the use of additional, more expressive flows, and perform more extensive numerical experiments validating and showcasing the method. The `harmonic`[2] Python package implementing the learned harmonic mean estimator, including with normalizing flows, is publicly available.

While normalizing flows can learn a normalized posterior density by definition, the normalization constant itself, *i.e.* the Bayesian evidence, is not directly accessible. Nevertheless, the Bayesian evidence can be computed by backing out the normalization constant, as discussed in Spurio Mancini et al. (2023), by taking the ratio of the unnormalized posterior (given by the product of the likelihood and prior) with the normalizing

flow representing a surrogate for the posterior. This approach, which we call the naïve normalizing flow estimator in Spurio Mancini et al. (2023), is highly dependent on the accuracy of the approximating normalizing flow and suffers a large variance, as discussed in Spurio Mancini et al. (2023). For comparison, we compute this naïve estimator in the current article and demonstrate its large variance. Very recently, Srinivasan et al. (2024) adopt this naïve estimator and attempt to reduce its variance by introducing an additional term in the loss that penalizes variability when training the flow. While this reduces the variability of the estimator, the estimator nevertheless remains highly dependent on the accuracy of the approximating flow and there is no guarantee that resulting evidence estimates are unbiased. Training flows using the forward Kullback-Leibler (KL) divergence when given samples from the target distribution is known to suffer from mode seeking behaviour, where the learned flow has narrower tails than the target (e.g. Murphy 2022). While the approach presented in Srinivasan et al. (2024) suffers from this problem as it directly impacts the accuracy of estimated evidence values, our learned harmonic mean estimator does not. Firstly, in the learned harmonic mean approach the internal importance sampling target distribution that is learned should in any case have narrower tails than the posterior. Secondly, the distribution that is learned in our approach is not used as a surrogate for the posterior so it need not be an accurate approximation. For further details see Section 2.3 or McEwen et al. 2021.

The remainder of this article is structured as follows. In Section 2 we briefly review Bayesian model comparison, the original harmonic mean estimator, elucidating its catastrophic failure arising from its large variance, and the learned harmonic mean estimator, which solves this large variance problem. In Section 3 we describe normalizing flows and how they can be integrated elegantly into the learned harmonic mean framework to provide a more robust, flexible and scalable approach than the simple machine learning models considered previously. In Section 4 we present numerical experiments that validate the effectiveness of our method. This includes low-dimensional benchmark examples where the ground truth value is accessible and a higher-dimensional practical cosmological example on DES-like simulations, as discussed above, where we validate against the evidence value computed by nested sampling. Finally, in Section 5 we present concluding remarks.

2. THE HARMONIC MEAN ESTIMATOR

In this section we briefly review Bayesian model comparison, the original harmonic mean estimator, and the learned harmonic mean estimator. We discuss the exploding variance problem of the original harmonic mean and describe how the learned harmonic mean solves this problem.

2.1. *Bayesian model comparison*

Using empirical data to test theoretical models lies at the heart of the scientific method, the foundation of research progress and innovation. Bayesian model comparison is a powerful approach for evaluating the relative plausibility of competing models in the light of data. In

---

[1] A notable exception that is applicable to high-dimensional settings is proximal nested sampling (Cai et al. 2022), although it is only applicable for log-convex likelihoods.

[2] https://github.com/astro-informatics/harmonic

the Bayesian framework probability distributions provide a quantification of uncertainty.

Bayes' theorem is a fundamental principle in Bayesian statistics that allows us to update our beliefs about models in light of observed data. Consider observed data y described through a model M parametrised by θ. Bayes' theorem gives us the posterior $p(\theta \,|\, y, M)$, the probability density of a model's parameter θ given observed data y and model M. It is expressed in terms of the prior probability density of the model, the likelihood of the data under that model, and the Bayesian evidence for the data:

$$p(\theta \,|\, y, M) = \frac{p(y \,|\, \theta, M)p(\theta \,|\, M)}{p(y \,|\, M)} = \frac{\mathcal{L}(\theta)\pi(\theta)}{z}. \quad (1)$$

The likelihood $p(y \,|\, \theta, M) = \mathcal{L}(\theta)$ expresses how probable the observed data y is for different values of the parameter θ. The prior $p(\theta \,|\, M) = \pi(\theta)$ quantifies pre-existing knowledge or assumptions about θ. The Bayesian evidence, also called the marginal likelihood, $p(y \,|\, M) = z$ is a normalizing factor for the posterior distribution.

The Bayesian evidence is often omitted when estimating parameters, for instance using MCMC methods, as only the relative values of the posterior probability are of interest. However, it is a crucial quantity in Bayesian model comparison. It quantifies the probability of observing the data under a particular model, integrating over the model's parameter space:

$$z = p(y \,|\, M) = \int \mathrm{d}\theta \, p(y \,|\, \theta, M)p(\theta \,|\, M) = \int \mathrm{d}\theta \, \mathcal{L}(\theta)\pi(\theta). \quad (2)$$

The Bayesian evidence can be used to compute Bayes' factors to provide a direct measure of the relative support for one model over another. The Bayes' factor between two models M_1, M_2 is defined as

$$\mathrm{BF}_{12} = \frac{p(y \,|\, M_1)}{p(y \,|\, M_2)}. \quad (3)$$

Given prior model probabilities, Bayes' factors offer a straightforward way to compare models and help make informed decisions about model selection.

In practice, the Bayesian evidence can be very challenging to calculate as θ is often high-dimensional. As a result, computing z involves evaluating a multidimensional integral over a potentially highly varied function. In principle, this could be done through a standard MCMC integration of the posterior, but this approach is not accurate in practice, even in relative low dimensions. Many alternative methods have been proposed; for reviews see Friel & Wyse (2012); Clyde et al. (2007). The most popular method for computing the evidence, particularly in the astrophysics community, is nested sampling Skilling (2006). As discussed already, many highly effective nested sampling algorithms have been developed. However, nested sampling imposes strong constraints on the method used to generate samples, significantly reducing its flexibility. Consequently, custom nested sampling algorithms must be designed and are typically restricted to relatively low dimensional settings.

2.2. *The original harmonic mean estimator*

The original harmonic mean estimator of the Bayesian evidence was introduced by Newton & Raftery (1994), providing an expression for the reciprocal Bayesian evidence $\rho = z^{-1}$ given by

$$\rho = \mathbb{E}_{p(\theta \,|\, y)}\left[\frac{1}{\mathcal{L}(\theta)}\right]. \quad (4)$$

This motivates the harmonic mean estimator $\hat{\rho}$ of the reciprocal Bayesian evidence, which can be written as an expectation of the reciprocal of the likelihood under the posterior,

$$\hat{\rho} = \frac{1}{N} \sum_{i=1}^{N} \frac{1}{\mathcal{L}(\theta_i)}, \quad \theta_i \sim p(\theta \,|\, y). \quad (5)$$

The Bayesian evidence can then be straightforwardly obtained as the inverse $\hat{z} = \hat{\rho}^{-1}$ (although a more accurate estimator of the evidence from its reciprocal can also be considered; McEwen et al. 2021). In principle, this estimator provides a simple and flexible method of evaluating the Bayesian evidence.

However, it was quickly realised that the harmonic mean estimator can be highly inaccurate due to its variance growing very large (Neal 1994; Clyde et al. 2007; Friel & Wyse 2012). The reason for this can be seen when interpreting the harmonic mean estimator through the lens of importance sampling (e.g. McEwen et al. 2021). Equation (4) can be rewritten as

$$\rho = \int \mathrm{d}\theta \, \frac{1}{z} \frac{\pi(\theta)}{p(\theta \,|\, y)} \, p(\theta \,|\, y). \quad (6)$$

It is clear that this expectation is equivalent to importance sampling, where the target density is the prior $\pi(\theta)$ and the sampling density is the posterior $p(\theta \,|\, y)$. This is in contrast to the typical importance sampling use case, where the posterior is the target distribution. For importance sampling to be effective, the sampling density must have fatter tails than the target in order for the target parameter space to be explored efficiently. If this condition is not fulfilled, the variance of the expectation becomes large. In the case of the harmonic mean estimator, the target density (prior) will normally have fatter tails than the sampling density (posterior). This is because the posterior gets updated with new information about the model encoded in the data, and as a result becomes narrower. Thus, the original harmonic mean estimator suffers from an exploding variance issue and is often inaccurate.

2.3. *Learned harmonic mean estimator*

One strategy to remedy the exploding variance problem of the harmonic mean estimator was proposed by Gelfand & Dey (1994), where an arbitrary normalized density $\varphi(\theta)$ is introduced to rewrite the expectation in Equation (4) as

$$\rho = \mathbb{E}_{p(\theta|y)}\left[\frac{\varphi(\theta)}{\mathcal{L}(\theta)\pi(\theta)}\right], \quad (7)$$

which naturally results in the estimator

$$\hat{\rho} = \frac{1}{N} \sum_{i=1}^{N} \frac{\varphi(\theta_i)}{\mathcal{L}(\theta_i)\pi(\theta_i)}, \quad \theta_i \sim p(\theta|y). \quad (8)$$

The density $\varphi(\theta)$ now takes the role of the importance sampling target. This estimator can therefore remedy the exploding variance problem provided that the target density $\varphi(\theta)$ is selected so that it is contained within the posterior. However, this condition is not trivial to enforce, especially in high dimensions since there is a trade-off between accuracy and efficiency. The contribution to the estimator from each posterior sample θ_i is weighted by the target density $\varphi(\theta_i)$. Low weights reduce the contribution of the posterior sample to the estimator, reducing its effective sample size and thus efficiency. However, the alternative of avoiding low weights can result in a target $\varphi(\theta)$ that is not contained within the posterior, giving rise to the exploding variance problem. In prior work, a multivariate Gaussian has been considered Gelfand & Dey (1994), although this often fails to contain $\varphi(\theta)$ within the posterior (Chib 1995; Clyde et al. 2007). Indicator functions have also been considered (Robert & Wraith 2009; van Haasteren 2014), although typically result in low efficiency. Other solutions to this problem have been proposed but they can be inaccurate, inefficient or limited in their use cases (Chib 1995; Lenk 2009; Raftery et al. 2006).

The learned harmonic mean estimator was proposed recently by some of the authors of the current article (McEwen et al. 2021), where machine learning methods are used to solve the exploding variance problem of the original harmonic mean. It was realized by McEwen et al. (2021) that the optimal target density is the normalized posterior, i.e.

$$\varphi^{\text{optimal}}(\theta) = \frac{\mathcal{L}(\theta)\pi(\theta)}{z}. \tag{9}$$

By definition of the problem, however, the normalized posterior is not accessible as the normalization factor is the Bayesian evidence itself. However, the target does not need to be a close approximation of the posterior for the estimate to be correct. It is more important for the target's probability mass to be contained within the posterior to avoid the variance becoming large. McEwen et al. (2021) develop a bespoke optimization approach that learns the posterior density from its samples while ensuring that the resulting model satisfies this condition. They also derive an unbiased estimator of the variance of the estimator and the variance of the variance, which are empirically shown to be accurate. The estimate of the Bayesian evidence computed with the learned harmonic mean thus comes with an error estimate, which can give an indication of how confident one should be in the result, and a number of additional sanity checks (McEwen et al. 2021).

The learned harmonic mean results in an accurate estimator of the Bayesian evidence that is agnostic to the sampling strategy, just like the original harmonic mean. This property ensures flexibility of the method, meaning it can be used in conjunction with efficient MCMC sampling techniques and variational inference approaches. The learned harmonic mean has been shown to be highly accurate on numerous example problems, including several cases where the original harmonic mean had been shown to fail catastrophically (Clyde et al. 2007; Friel & Wyse 2012). However, the bespoke training approach requires an appropriate model to be cho-

sen carefully and the hyperparameters to be fine-tuned through cross validation. Moreover, the simple machine learning models considered previously do not scale well to high-dimensional settings.

3. LEARNED HARMONIC MEAN ESTIMATOR WITH NORMALIZING FLOWS

In this section we describe the learned harmonic mean with normalizing flow for estimation of the Bayesian evidence. Normalizing flows can be elegantly coupled with the learned harmonic mean to provide an approach that is more robust, flexible and scalable than the machine learning models considered previously.

3.1. Normalizing flows

Normalizing flows meet the core requirements of the learned target distribution of the learned harmonic mean estimator: namely, they provide a normalized probability distribution for which one can evaluate probability densities. Flows are a class of machine learning model, where an underlying probability distribution is learned, e.g., from training data. The learned distribution can then be sampled from, generating new data instances similar to those in the training set. The learned approximation of the probability density is also accessible, and it is normalized, which is crucial for our use.

Normalizing flow models work by transforming a simple base distribution into a more complex distribution through a series of bijections (invertible transformations). For a comprehensive review of normalizing flows we refer the reader to Papamakarios et al. (2021). The base distribution is chosen so that it is easy to sample from and to evaluate its probability density, typically a Gaussian with unit variance. A vector θ of an unknown distribution $p(\theta)$, can be expressed through a transformation B of a latent vector u sampled from the base distribution $q(u)$:

$$\theta = B(u), \text{ where } u \sim q(u). \tag{10}$$

B must be invertible and B and its inverse B^{-1} must be differentiable. When these conditions are satisfied, we can simply calculate the density of the distribution of θ through the change of variables formula by

$$p(\theta) = q(u)|\det J_B(u)|^{-1}, \tag{11}$$

where $J_B(u)$ is the Jacobian corresponding to B. Such transformations are composable: $p(\theta)$ can be transformed again, and the resulting normalized density can be obtained analogously. In practice B consists of a series of transformations. These are often defined in such a way that the determinant of $J_B(u)$ can be computed efficiently. This is where the power of normalizing flows lies – a simple base distribution, when taken through a series of simple transformations can become much more expressive and is able to approximate complex targets. In reality, the resulting distribution is an imperfect approximation of $p(\theta)$ that we call $p_{\text{NF}}(\theta, \beta)$, where β denotes the trainable parameters of the transformations.

A multitude of flow architectures with different strengths have been proposed. In this work (and in the `harmonic` code), we use real-valued non-volume preserving (Dinh et al. 2017) and rational quadratic spline flows

(Durkan et al. 2019). However, any flow model can be integrated into the method, offering greater computational scalability.

3.1.1. *Real non-volume preserving flows*

Real-valued non-volume preserving (real NVP) flows were introduced by Dinh et al. (2017). Their architecture is relatively simple, consisting of a series of affine coupling layers. Consider the D dimensional input x, split into elements up to and following d, respectively, $x_{1:d}$ and $x_{d+1:D}$, for $d < D$. Given input x, the output y of an affine couple layer is calculated by

$$y_{1:d} = x_{1:d}; \tag{12}$$

$$y_{d+1:D} = x_{d+1:D} \odot \exp\big(s(x_{1:d})\big) + t(x_{1:d}), \tag{13}$$

where $\odot$ denotes Hadamard (elementwise) multiplication, and the scale s and translation t are neural networks with trainable parameters. The Jacobian of such a transformation is a lower-triangular matrix, making its determinant efficient to calculate.

3.1.2. *Rational quadratic spline flows*

A more complex and expressive class of flows are rational quadratic spline flows introduced by Durkan et al. (2019). The architecture is similar to real NVP flows, but the layers include monotonic splines. These are piecewise functions consisting of multiple segments of monotonic rational quadratics with learned parameters. Given input x, the output y of a rational quadratic coupling layer has the form:

$$\alpha_{1:d} = \text{Trainable parameters}; \tag{14}$$

$$\alpha_{d+1:D} = n(x_{1:d}); \tag{15}$$

$$y_i = g_{\alpha_i}(x_i), \tag{16}$$

where n is a neural network and g_{α_i} is a spline parametrised by α_i, with each bin defined by a monotonically-increasing rational-quadratic function. Such layers are combined with alternating affine transformations to create the normalizing flow. Thanks to their more expressive and sophisticated architecture, rational quadratic spline flows are well-suited to higher dimensional and more complex problems than real NVP flows (Durkan et al. 2019).

3.2. *The learned harmonic mean estimator with normalizing flows*

In this work we address the limitations of the simple machine learning methods considered in the learned harmonic mean framework previously. Recall, the aim is to learn an approximation of the posterior from samples but with the critical constraint that the tails of the learned distribution are contained within the posterior. To learn appropriate models a bespoke optimization algorithm was considered in McEwen et al. (2021). Normalizing flows afford an elegant alternative solution for keeping the learned target density contained within the posterior, rendering the bespoke training approach unnecessary. The importance sampling target density is first learned using a normalizing flow model and then concentrated by reducing the variance of the base distribution, i.e. reducing its "temperature". The resulting
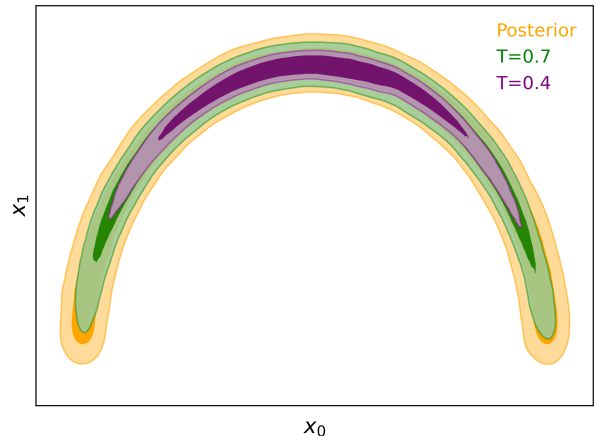

Fig. 1.— Diagram illustrating how reducing the temperature parameter concentrates the probability density of a normalizing flow. The trained flow at $T = 1$ is a normalized approximation of the posterior distribution. The variance of the base distribution, which we call the temperature parameter $T \in (0,1)$, is reduced, concentrating the probability density of the transformed distribution. This ensures that it is contained within the posterior, which is a necessary condition for the internal learned importance target distribution of the learned harmonic mean estimator.

method provides an improved estimator of the Bayesian evidence that retains the flexibility and accuracy of its predecessor, while improving its robustness and scalability.

3.2.1. *Training the flow*

Before we estimate the evidence we need to train a normalizing flow on samples from the posterior. When training normalizing flows, the forward KL divergence is well-suited as the loss function L when we have samples of the target distribution. Consider an unknown posterior distribution of interest $p(\theta)$ and its approximating flow $p_{\text{NF}}(\theta, \beta)$, where β are the trainable flow parameters. The KL divergence can be interpreted as a measure of the dissimilarity between $p(\theta)$ and $p_{\text{NF}}(\theta, \beta)$ and is therefore a natural quantity to minimize when training a normalizing flow. The forward KL divergence between the two distributions can be expressed as

$$L(\beta) = D_{KL}\left[\, p(\theta)\,||\,p_{\text{NF}}(\theta, \beta)\,\right]$$

$$= -\,\mathbb{E}_{p(\theta)}\left[\log\big(\,p_{\text{NF}}(\theta, \beta)\,\big)\right] + \text{const.} \tag{17}$$

Given N samples θ_i from the posterior, where $i = \{1, \ldots, N\}$, the expectation in Equation (17) can be approximated by Monte Carlo as

$$L(\beta) \approx -\frac{1}{N}\sum_{i=1}^{N} \log\big(\,p_{\text{NF}}(\theta_i, \beta)\,\big) + \text{const.} \tag{18}$$

Minimizing this approximation is equivalent to fitting the normalizing flow to the samples by maximum likelihood (Papamakarios et al. 2021). We take this approach to trainining our flow, and minimize the loss given by Equation (18) using the Adam optimizer (Kingma & Ba 2017; Dozat 2016). We use a portion of the samples for training the flow and reserve the rest to be used for inference, to be substituted when estimating the evidence.

It is worth stressing that this is the standard training approach for normalizing flows. By replacing the simple

machine learning methods considered in McEwen et al. (2021) with flows, we render their bespoke training approach unnecessary, making the method more robust and flexible.

As discussed in Section 1, training a flow by forward KL divergence, or equivalently maximum likelihood, can suffer from mode seeking behaviour, where the learned flow has narrower tails than the target (e.g. Murphy 2022). Nevertheless, this is not a problem for use of the flow in the learned harmonic estimator since we seek a learned distribution that has narrower tails than the posterior. Moreover, the learned distribution is not used as a surrogate for the posterior but rather as the importance sampling target. The learned distribution need not be a highly accurate approximation of the posterior but it critically must be concentrated within the posterior. Consequently, the mode seeking behaviour of training normalizing flows by forward KL divergence does not compromise the learned harmonic mean estimator.

3.2.2. *Concentrating the probability density*

Once the flow is trained on samples from the posterior, we concentrate its probability density by reducing what we call the flow temperature parameter T. This is a factor $T \in (0, 1)$ by which the variance of the base Gaussian distribution is multiplied. Reducing the base distribution's variance has the effect of concentrating its probability density in parameter space, or reducing its "temperature" in a statistical mechanics interpretation. This has the effect of also concentrating the probability density of the transformed distribution due to the continuity and differentiability of the flow, as illustrated in Figure 1. Hence, the concentrated flow is the perfect candidate for the importance sampling target in the harmonic mean estimator, as it is normalized and close to the posterior but contained within it. After a flow is trained, it can be used in the learned harmonic mean estimator with different temperature values without the need to retrain for each T.

3.2.3. *Standardization*

We standardize the training and inference data. We calculate the mean and variance of the input training data represented in a matrix Θ^{train} and remove that before fitting the model. This means that each entry of the data matrix is transformed as

$$\Theta_{ij}^{\text{train}} \mapsto (\Theta_{ij}^{\text{train}} - \overline{\Theta}_j^{\text{train}})/\sigma_j^{\text{train}}, \qquad (19)$$

where $\overline{\Theta}_j^{\text{train}}$ is the mean and σ_j^{train} is the standard deviation of the training data parameter column j (calculated over the data points). This training data consists of samples from the parameter space so $j \in 1, \ldots, D$, where D is the dimension of θ. We then apply this same transformation, with $\overline{\Theta}^{\text{train}}$ and σ^{train} vectors kept the same, to the data points for which we are predicting the probability density, namely the inference data. For the density to still be normalized, we need to then also multiply the flow density by the Jacobian of this transformation, so the predicted density for a standardized model $p_{\text{NF}}^S(\theta)$ is

$$p_{\text{NF}}^S(\theta) = p_{\text{NF}}(\theta) \prod_{j=1}^{D} (\sigma_j^{\text{train}})^{-1}. \qquad (20)$$

3.2.4. *Evidence error estimate*

In addition to an estimate of the evidence itself, we also require an estimate of its error. In McEwen et al. (2021) approaches are proposed to estimate the variance of the learned harmonic mean estimator and also its variance. Specifically, the Bayesian evidence estimate and its error are considered $\hat{\rho} \pm \hat{\sigma}$. While quoting these terms is sufficient for many toy problems, to ensure numerical stability for practical problems in higher dimensions it is necessary to always work in log space to avoid numerical overflow. Converting the error estimate $\hat{\sigma}$ to log space is non-trivial as $\log(\text{var}(x)) \neq \text{var}(\log(x))$ in general. To remain in log space we are interested in the log-space error $\hat{\zeta}_\pm$ defined by

$$\log(\hat{\rho} \pm \hat{\sigma}) = \log(\hat{\rho}) + \hat{\zeta}_\pm. \qquad (21)$$

The log-space error estimate can be computed by

$$\hat{\zeta}_\pm = \log(\hat{\rho} \pm \hat{\sigma}) - \log(\hat{\rho}) = \log(1 \pm \hat{\sigma}/\hat{\rho}), \qquad (22)$$

where

$$\hat{\sigma}/\hat{\rho} = \exp(\log(\hat{\sigma}) - \log(\hat{\rho})). \qquad (23)$$

This way we can avoid computing $\hat{\rho} \pm \hat{\sigma}$ directly. We only compute $\log(\hat{\sigma}) - \log(\hat{\rho})$, which we expect to be much smaller and less susceptible to overflow. When quoting the result with log-space errors we use the notation $\log(\hat{\rho})_{\hat{\zeta}_-}^{\hat{\zeta}_+}$. The log evidence errors can be straightforwardly obtained by swapping the negative and positive errors of the reciprocal log evidence.

3.2.5. *Code*

The learned harmonic mean estimator with normalizing flows is implemented in the `harmonic` package[3], from version 1.2.0 onwards. The methodology described in this section, with real NVP and rational quadratic spline flows, has been implemented in JAX and is available in recent releases of `harmonic` on PyPi and GitHub. Furthermore, other parts of the `harmonic` code have been updated to run on JAX, which is a Python package offering acceleration, just-in-time compilation and automatic differentiation functionality (Bradbury et al. 2018). Consequently, `harmonic` can now be run on hardware accelerators such as GPUs, potentially reducing computation times and allowing the user to tackle more complex, computationally demanding problems. Additionally, the automatic differentiation functionality opens up the possibility of optimizing based on evidence (e.g. for experimental design), as gradients are now accessible all the way down to evidence level, which provides an intriguing avenue for further research. The normalizing flow portion of the code is implemented using the `flax` (Heek et al. 2023), TensorFlow Probability (Dillon et al. 2017), `optax` and `distrax` (DeepMind et al. 2020) packages.

3.2.6. *Naïve Bayesian evidence estimation using normalizing flows*

As discussed in Section 1, and first described in Spurio Mancini et al. (2023), since flows are normalized it is

---

[3] https://github.com/astro-informatics/harmonic

possible to back out their normalizing constant to provide an estimate of the Bayesian evidence. We recall this approach here for reference.

Given samples θ_i an estimate of the evidence can be computed for each sample by

$$z_i = \frac{\mathcal{L}(\theta_i)\pi(\theta_i)}{p_{\mathrm{NF}}(\theta_i)}. \tag{24}$$

While posterior samples are typically available and hence used, in principle the samples θ_i do not necessarily need to be drawn from the posterior. An overall estimate of the evidence and its spread can then simply be computed from the mean of these evidence estimates and their standard deviation. However, the resulting evidence estimator is likely to be biased and will have a large variance. This is because it is highly dependent on the accuracy of the learned normalizing flow, which is used as a surrogate for the posterior, as discussed in Section 1. The learned harmonic mean does not suffer from these issues.

4. NUMERICAL EXPERIMENTS

To validate the effectiveness of the method presented in this paper, we perform a series of numerical experiments. Firstly, in Section 4.2 we repeat a series of low-dimensional benchmark problems performed by McEwen et al. (2021) but using normalizing flows to learn the importance sampling target. The underlying examples are described in more detail by McEwen et al. (2021). The original harmonic mean estimator has been shown to fail catastrophically for many of these examples (Friel & Wyse 2012), while our learned harmonic mean remains accurate. In Section 4.3 we study the impact of varying the temperature parameter on the evidence estimate, showing the robustness of our method. Then in Section 4.4 we present a practical application of our method in a cosmological context for the DES (Dark Energy Survey). We perform a joint lensing-clustering analysis ("3x2pt") on a DES Y1-like configuration. We compare our results with the values obtained through the conventional method of nested sampling.

4.1. *Architectures, sampling and training*

In the experiments where a real NVP flow is used, translation networks of the affine coupling layers are given by two-layer dense neural networks with a leaky ReLU activation function in between. For the scaling layers this is scaled by another dense layer with a softplus activation. We permute the inputs between coupling layers to ensure the flow transforms all elements. In the low dimensional benchmark experiments we consider a real NVP flow, unless otherwise stated, with six coupling layers, where typically only the first two include scaling. When we use a rational quadratic spline flow, it has a range -10 to 10 (outside of this range it defaults to a linear transformation). The conditioner for the spline hyperparameters is a multi-layer perceptron with a tanh activation. We use a Gaussian base distribution with zero mean and an identity covariance matrix for all flows.

For the low-dimensional benchmark examples, we generate samples from the posterior using MCMC methods implemented in the `emcee` package (Foreman-Mackey et al. 2013). In the practical cosmological example, we use the Metropolis-Hastings sampling approach
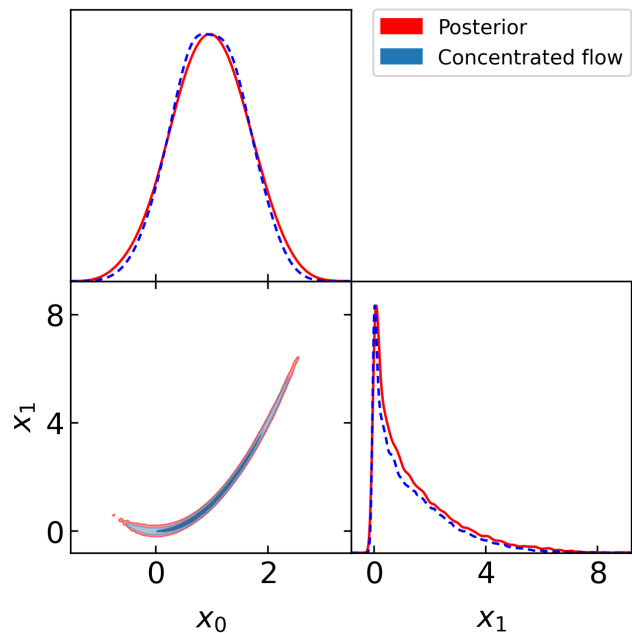

FIG. 2.— Corner plot of the sampled posterior (solid red) and a real NVP flow with temperature $T = 0.9$ (dashed blue) for the Rosenbrock benchmark problem. The internal importance target distribution of the estimator given by the concentrated flow is contained within the posterior, as required for the learned harmonic mean estimator.

(Metropolis et al. 1953; Hastings 1970) implemented in the `cobaya` package (Torrado & Lewis 2019). We then train the flow on half of the samples by maximum likelihood and use the remaining samples for inference.

4.2. *Benchmark examples*

4.2.1. *Rosenbrock*

The Rosenbrock problem is a common benchmark example considered when estimating the Bayesian evidence. The Rosenbrock distribution's narrow curving degeneracy presents a challenge in sufficiently exploring the resulting posterior distribution to accurately evaluate the Bayesian evidence. The Rosenbrock function is given by

$$f(x) = \sum_{i=1}^{d-1} \left[100(x_{i+1} - x_i^2)^2 + (x_i - 1)^2 \right], \tag{25}$$

where d denotes the number of dimensions. In our example we consider a 2-dimensional problem with the log-likelihood given by $\log \mathcal{L}(x) = -f(x)$ and a uniform prior $x_0 \in [-10, 10]$ and $x_1 \in [-5, 15]$.

We draw $1,500$ samples for 200 chains, with burn-in of 500 samples, yielding $1,000$ posterior samples per chain. Figure 2 shows the corner plot of samples from the posterior (solid red line) and a real NVP flow with 2 scaled and 4 unscaled layers at temperature $T = 0.9$ (dashed blue line). It can be seen that the flow approximates the posterior quite well while remaining contained within it. This is exactly what we want in a target distribution for the harmonic mean estimator.

Figure 3a shows a violin plot of the results of this experiment repeated 100 times with posterior samples generated from different seeds. The ground truth obtained

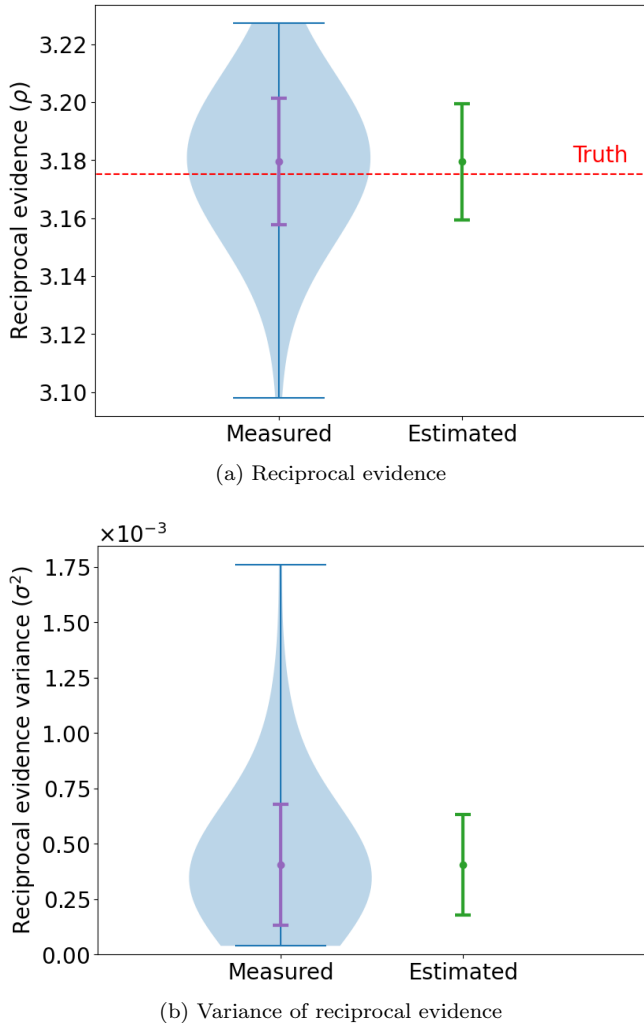(a) Reciprocal evidence

(b) Variance of reciprocal evidence

FIG. 3.— Violin plots of the reciprocal Bayesian evidence computed by the learned harmonic mean estimator for the Rosenbrock benchmark problem repeated 100 times. (a) Reciprocal Bayesian evidence estimates across runs (measured) along with the estimate of the standard deviation computed by the error estimator (estimated). The ground truth is shown in red. (b) Sample variance of the estimator across runs (measured) alongside the standard deviation computed by the variance-of-variance estimator (estimated). The evidence estimates and their error estimators are highly accurate.

through numerical integration is shown in red. It can be seen that the evidence values estimated using our method are accurate, agreeing with the ground truth value. It can also be seen that the estimator of the population variance agrees with the variance measured across the repeats. Figure 3b shows a violin plot of the variance estimator across runs alongside the standard deviation calculated from the variance-of-variance estimator. It can be seen they are also in agreement. The Bayesian evidence estimates obtained using the learned harmonic mean and their error estimates are highly accurate.
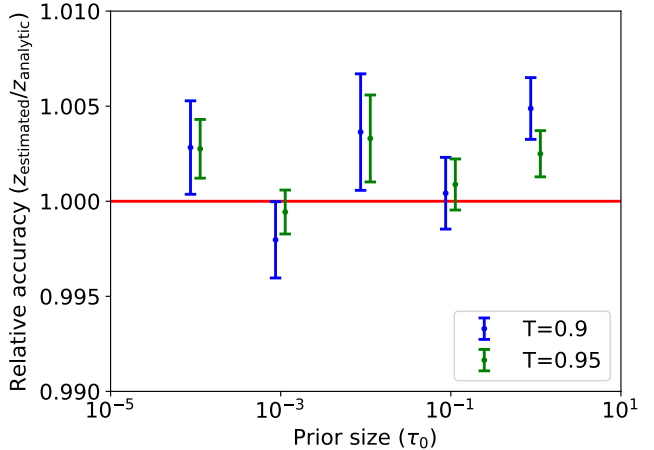
4.2.2. *Normal-Gamma*

We also consider the Normal-Gamma model (Bernardo & Smith 1994) where data are distributed normally

$$y_i \sim N(\mu, \tau^{-1}), \tag{26}$$
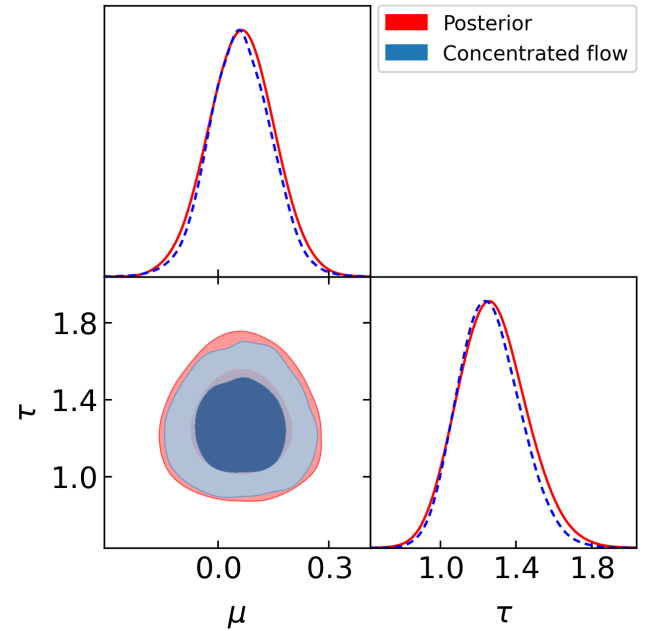
(a) Corner plot for the Normal-Gamma example with $\tau_0 = 0.001$

(b) Estimate accuracy for varying prior sizes

FIG. 4.— (a) Corner plot of the sampled posterior (solid red) and real NVP flow with temperature $T = 0.9$ (dashed blue) for the Normal-Gamma example with $\tau_0 = 0.001$. The internal importance target distribution given by the concentrated flow is contained within the posterior, as required for the learned harmonic mean estimator. (b) Ratio of Bayesian evidence values computed by the learned harmonic mean estimator with a concentrated flow to those computed analytically for the Normal-Gamma problem with error bars corresponding to the estimated standard deviation. Bayesian evidence estimated with a flow at temperature $T = 0.9$ (blue) and $T = 0.95$ (green) are shown, with slight offsets for ease of visualization. Unlike the original harmonic mean, our method produces accurate estimates which are sensitive to prior size.

for $i \in \{1, \ldots, n\}$, with mean μ and precision τ. A normal prior is assumed for μ and a Gamma prior for τ:

$$\mu \sim N(\mu_0, (\tau_0\tau)^{-1}), \tag{27}$$
$$\tau \sim Ga(a_0, b_0), \tag{28}$$

with mean $\mu_0 = 0$, shape $a_0 = 10^{-3}$ and rate $b_0 = 10^{-3}$. The precision scale factor τ_0 controls how diffuse the prior is. Friel & Wyse (2012) apply the original har-

monic mean for this example and show that the evidence estimate does not vary with τ_0, unlike the analytic ground truth value. We repeat this experiment, drawing $1,500$ samples for 200 chains, with burn in of 500 samples, yielding $1,000$ posterior samples per chain. We use a real NVP flow with 2 scaled and 4 unscaled layers at temperatures $T = 0.9$ and $T = 0.95$ to estimate the evidence.

Figure 4a shows an example corner plot of the training samples from the posterior for $\tau = 0.001$ (red) and from the normalizing flow (blue) at temperature $T = 0.9$. Again, it can be seen that the concentrated learned target is close to the posterior but with thinner tails, as is required.

Figure 4b shows the relative accuracy of the evidence estimate computed using our method for a range of prior sizes. It can be seen that, unlike the original harmonic mean estimator, our method is accurate for a range of τ_0. Results are computed with the trained flow at temperature $T = 0.9$ (blue) and $T = 0.95$ (green). They are accurate in both cases, showing that the temperature parameter does not require fine-tuning.

4.2.3. *Logistic regression models: Pima Indian example*

We consider an example involving the comparison of two logistic regression models used to describe the Pima Indians data (Smith et al. 1988), originally from the National Institute of Diabetes and Digestive and Kidney Diseases.

This analysis was originally performed to study indicators of diabetes in $n = 532$ Pima Indian women. The predictors of diabetes considered included the number of prior pregnancies (NP), plasma glucose concentration (PGC), body mass index (BMI), diabetes pedigree function (DP) and age (AGE). The probability of diabetes p_i for person $i \in \{1, \ldots, n\}$ is modelled by the logistic function

$$p_i = \frac{1}{1 + \exp\left(-\theta^{\mathrm{T}} x_i\right)}, \qquad (29)$$

with covariates $x_i = (1, x_{i,1}, \ldots x_{i,d})^{\mathrm{T}}$ and parameters $\theta = (\theta_0, \ldots, \theta_d)^{\mathrm{T}}$, where d is the total number of covariates considered. The likelihood is given by

$$\mathcal{L}(y \mid \theta) = \prod_{i=1}^{n} p_i^{y_i} (1 - p_i)^{1-y_i}, \qquad (30)$$

where $y = (y_1, \ldots, y_n)^{\mathrm{T}}$ is the diabetes incidence with y_i equal to one if patient i has diabetes and zero otherwise. The prior distribution on θ is a Gaussian with precision $\tau = 0.01$.

Two such logistic regression models are considered:

Model M_1 : covariates = {NP, PGC, BMI, DP};

Model M_2 : covariates = {NP, PGC, BMI, DP, AGE},

where both additionally include a bias. We estimate the Bayes factor of these models BF_{12} with our method and compare it to a benchmark value computed by Friel & Wyse (2012) using a reversible jump algorithm (Green 1995). They obtain a value of $\mathrm{BF}_{12} = 13.96$ ($\log \mathrm{BF}_{12} = 2.636$), which we treat as ground truth. We draw $5,000$ samples for 200 chains, with burn in of $1,000$ samples, yielding $4,000$ posterior samples per chain. We use a
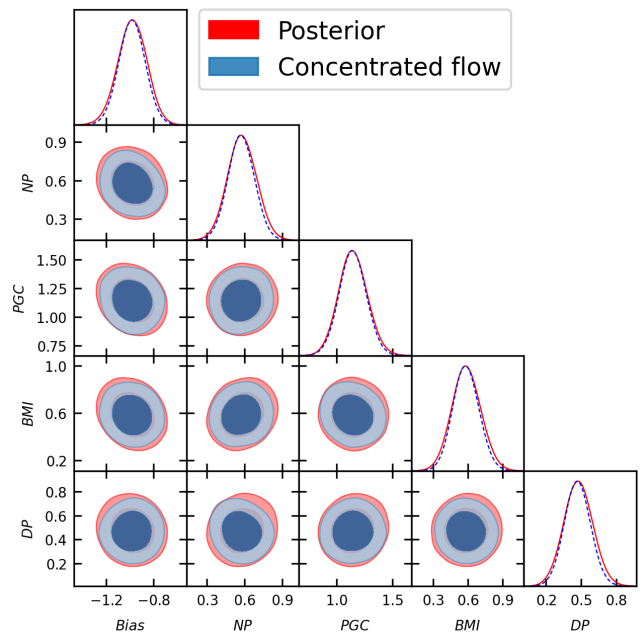
(a) Model 1
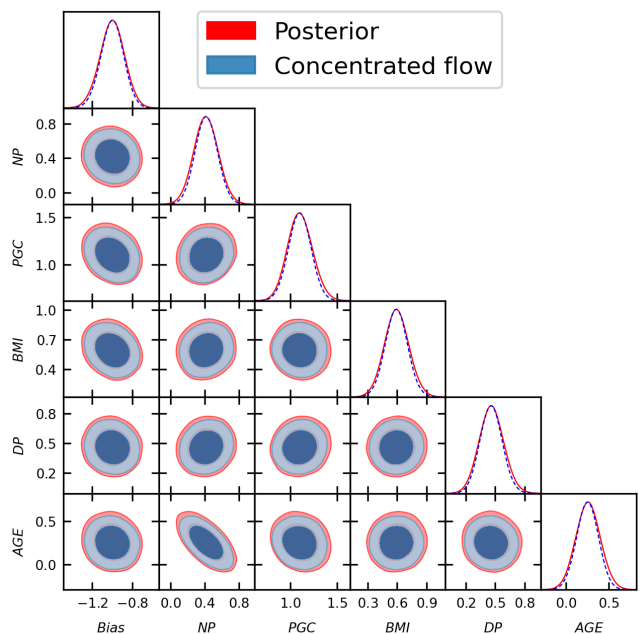
(b) Model 2

FIG. 5.— Corner plots of the sampled posterior (solid red) and real NVP flow trained on the posterior samples with temperature $T = 0.9$ (dashed blue) for the Pima Indian benchmark problem for $\tau = 0.01$. The dimensions correspond to parameters θ_i associated with the covariates included in the analysis. The internal importance target distribution given by the concentrated flow is contained within the posterior and has thinner tails, as required for the learned harmonic mean estimator.

real NVP flow with 2 scaled and 4 unscaled layers at temperature $T = 0.9$, applying standardization.

Figure 5 shows the corner plots for this example for both models. The training samples from the posterior are shown in red and from the normalizing flow at temperature $T = 0.9$ in blue. Once again, we see that the concentrated flow is contained within the posterior as

expected. The log evidence found for Model 1 and 2 is $-257.230^{0.003}_{-0.003}$ and $-259.857^{0.002}_{-0.002}$ respectively, resulting in the estimate $\log \mathrm{BF}_{12} = 2.627^{0.004}_{-0.004}$, indicating a slight preference for Model 1. The Bayes factor value is in close agreement with the benchmark, whereas the original harmonic mean estimator was not accurate (Friel & Wyse 2012).

4.2.4. Non-nested linear regression models: Radiata pine example

In the last benchmark example we compare two non-nested linear regression models describing the Radiata pine data (Williams 1959). The dataset consists of measurements of the maximum compression strength parallel to the grain y_i, density x_i and resin-adjusted density z_i, for specimen $i \in \{1, \ldots, n\}$. Two Gaussian linear models are compared, one with density and one with resin-adjusted density as variables:

$$\text{Model } M_1: \quad y_i = \alpha + \beta(x_i - \bar{x}) + \epsilon_i, \quad \epsilon_i \sim \mathrm{N}(0, \tau^{-1}); \tag{31}$$

$$\text{Model } M_2: \quad y_i = \gamma + \delta(z_i - \bar{z}) + \eta_i, \quad \eta_i \sim \mathrm{N}(0, \lambda^{-1}), \tag{32}$$

where $\bar{x}$, $\bar{z}$ denote the mean values of x_i and z_i respectively, and τ and λ denote the precision of the noise for the respective models. For both models, Gaussian priors with means $\mu_\alpha = 3000$ and $\mu_\beta = 185$, and precision scales $r_0 = 0.06$ and $s_0 = 6$ are chosen. A gamma prior is assumed for the noise precision with shape $a_0 = 3$ and rate $b_0 = 2 \times 300^2$. The evidence can be computed analytically for this example (McEwen et al. 2021).

Using emcee, we draw $10,000$ samples for 200 chains, with burn in of $2,000$ samples, yielding $8,000$ posterior samples per chain. We train a rational quadratic flow consisting of 2 layers, with 50 spline bins. Standardization is applied to the data as detailed in Section 3.2, which is necessary due to the vast difference in scale of the parameter dimensions.

Figure 6 shows a corner plot of the training samples from the posterior (red) and from the normalizing flow (blue) at temperature $T = 0.9$ for both models. Again, it can be seen that the concentrated learned target is contained within the posterior. The log evidence found for Model 1 and 2 is $-310.1284^{0.0007}_{-0.0007}$ and $-301.7044^{0.0008}_{-0.0008}$ respectively, resulting in the estimate $\log \mathrm{BF}_{12} = 8.424^{0.001}_{-0.001}$. The analytic values of the log evidence are -310.1283 and -301.7046 for Models 1 and 2 respectively, resulting in the estimate $\log \mathrm{BF}_{12} = 8.424$. The value obtained using our estimator is in close agreement with the ground truth. The learned harmonic mean gives an accurate estimate of the evidence, whereas the original harmonic mean estimator fails catastrophically for this example (Friel & Wyse 2012).

4.3. Robustness of the temperature parameter

Many methods of estimating the evidence require careful fine-tuning of hyperparameters. As explained in Section 2.3, this was also the case for the learned harmonic mean estimator when using the classical machine learning models as considered previously. The target distribution was learned using simple machine learning models and a bespoke optimization approach designed to ensure
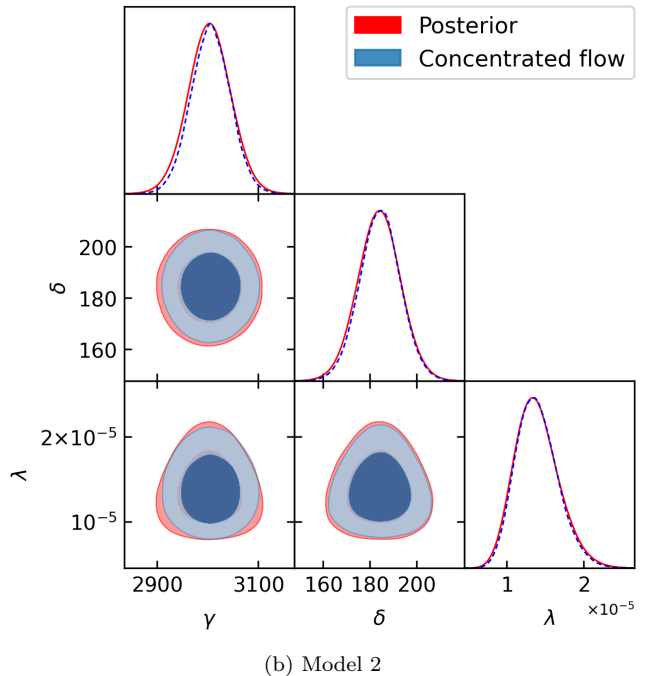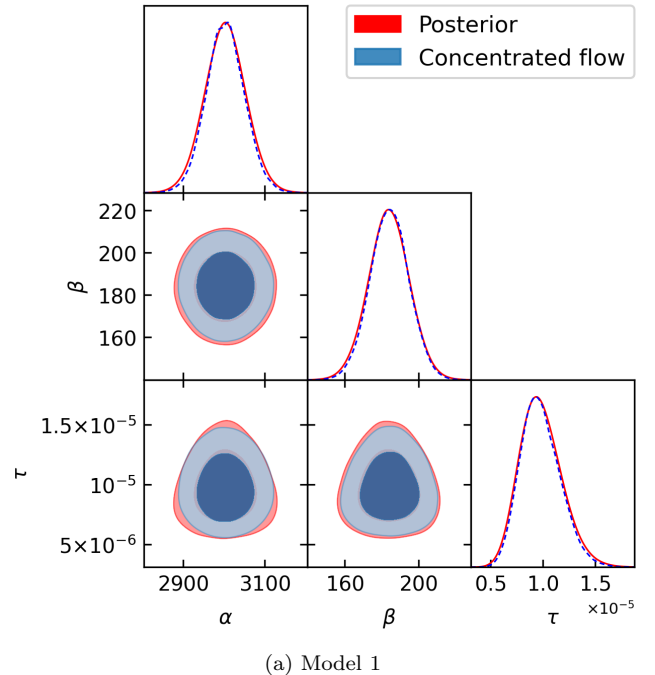

(a) Model 1

(b) Model 2

FIG. 6.— Corner plot of the the sampled posterior (solid red) and rational quadratic spline flow trained on the posterior samples with temperature $T = 0.9$ (dashed blue) for the Radiata pine benchmark problem. The internal importance target distribution given by the concentrated flow is contained within the posterior and has thinner tails, as required for the learned harmonic mean estimator.

the target distribution is contained within the posterior. The models had to be carefully chosen and their hyperparameters had to be fine-tuned for the estimator to be accurate and validated by cross-validation. In this work, through the introduction of a more sophisticated machine learning model, normalizing flows, we are able to avoid this drawback and create a more robust estimator.

Our learned harmonic mean estimator with normaliz-

TABLE 1
EVIDENCE AND BAYES FACTORS COMPUTED FOR DES Y1-LIKE 3X2PT ANALYSIS

Method	$\log(z_{\Lambda\text{CDM}})$	$\log(z_{w\text{CDM}})$	$\log \text{BF}_{\Lambda\text{CDM-}w\text{CDM}}$	Computation time (64 CPU cores)
Learned harmonic mean	$-65.262^{+0.011}_{-0.011}$	$-67.407^{0.009}_{-0.009}$	$2.145^{0.014}_{-0.014}$	16 hours (sampling) + 16 minutes (evidence)
Nested sampling	-65.21 ± 0.32	-67.44 ± 0.32	2.23 ± 0.45	94 hours (sampling and evidence)
Naïve flow estimator	-64.9 ± 0.8	-67.0 ± 1.1	2.1 ± 1.4	Similar to learned harmonic mean
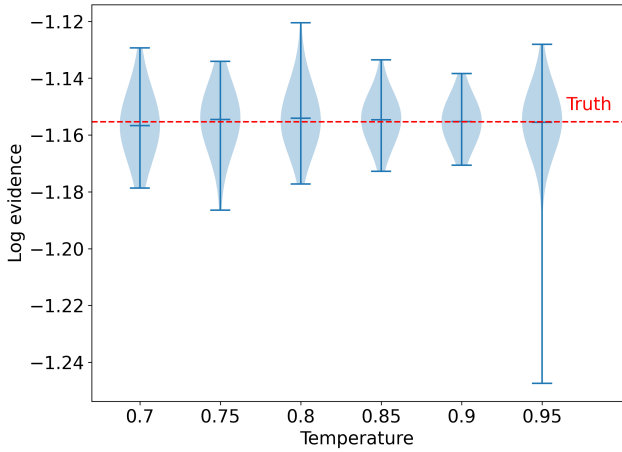
FIG. 7.— Impact of the temperature parameter value on the evidence estimate. The figure contains violin plots of the evidence estimates across runs for the Rosenbrock problem for a range of temperature values. The ground truth is shown in red. It can be seen that the Bayesian evidence estimates are accurate for a range of temperatures. This shows that the learned harmonic mean is a robust method and does not require careful parameter fine-tuning. The outlier value for $T = 0.95$ illustrates the fact that even though the corresponding concentrated flow better approximates the optimal importance target given by the posterior, a flow temperature closer to unity does not necessarily lead to a better estimate since as $T \to 1$ it is possible the flow may not contain the posterior (as it does not represent the true underlying posterior but only a learned approximation).

ing flows contains essentially just a single hyperparameter: the temperature T of the concentrated flow. We perform numerical experiments to study the influence of the temperature parameter T on the evidence estimate. The Rosenbrock benchmark problem is considered again, as described in Section 4.2.1. The experimental process is performed for a range of temperatures $T \in [0.7, 0.95]$, repeating it 100 times for each value. For each repeat, a new seed is used to generate a new dataset of posterior samples, and to initialize the optimizer.

Figure 7 shows violin plots of the log evidence estimates obtained in this experiment plotted for each temperature value. The ground truth, obtained through direct numerical integration is shown in red. It can be seen that the evidence estimates remain accurate and unbiased for the range of temperature values considered. This illustrates the robustness of our method – the temperature parameter does not need to be fine-tuned.

One must nevertheless ensure that the flow is indeed contained within the posterior as required for the learned harmonic mean to be accurate. The temperature parameter needs to be sufficiently small for this to be the case. If the flow was a perfect approximation of the posterior, any value $T \leq 1$ would do. In practice this is not the case, and if the temperature is chosen to be too close to unity, the flow might not be contained within the poste-

rior in some regions of the parameter space, causing the estimator's variance to grow. This effect can partially be seen when looking at the violin plot for $T = 0.95$ in Figure 7. Most of the evidence estimates remain accurate but it can be seen that there exists an outlier. The smallest evidence estimate computed is many standard deviations away from the ground truth. To avoid this, one should always ensure that the flow at the chosen temperature does not have fatter tails than the posterior. If the flow for $T = 1$ were a perfect approximation of the posterior, one would expect the variance of the estimator to increase as T is reduced below unity due to the resulting smaller effective sample size. However, when dealing with a finite number of samples from the posterior and imperfect approximations, a temperature value closer to unity is not always best. When T is large, the possibility of the flow not being contained within the posterior increases. It is better to choose a lower, more conservative value of T when dealing with a more complicated or high-dimensional posterior. In practice, we find $T \approx 0.9$ works well for most problems. A lower T value should be used if the posterior is particularly complex or high-dimensional. This value can then be adjusted based on the error estimate or other diagnostics computed by the `harmonic` code (McEwen et al. 2021).

4.4. *Practical cosmological example: DES Y1 analysis*

In Section 4.2 we showed that the learned harmonic mean estimator with normalizing flows works very well on a range of simple benchmark examples, where the ground truth Bayesian evidence is available. In this section we show it also performs well in a practical context, by applying it to a Dark Energy Survey Year 1 (DES Y1) example. DES is an on-going cosmological survey designed to gain insight into the nature of dark energy. We perform a 3x2pt analysis (Abbott et al. 2018a; Joachimi & Bridle 2010), i.e. a joint analysis of galaxy clustering and weak lensing considering shear, clustering and their cross correlation, on a DES Y1-like configuration.

We follow the reference approach described by Campagne et al. (2023), who extract and compress a subset of the DES Year 1 lensing and clustering data and set up a forward model following the DES Y1 Pipeline (Abbott et al. 2018a). We use the DES Y1 redshift distributions[4] and simulate a 3x2pt data vector for a fixed cosmology. We use this as our mock data vector and run an inference pipeline to obtain posterior contours and evidence estimates. We refer the reader to Campagne et al. (2023) for the priors and all other details. To sample from the posterior we use the `Cobaya` package (Torrado & Lewis 2019) with the Metropolis-Hastings algorithm. We then apply `harmonic` to these samples to evaluate the Bayesian evidence. For comparison, we also sample using

---

[4] http://desdr-server.ncsa.illinois.edu/despublic/y1a1_files/chains/2pt_NG_mcal_1110.fits
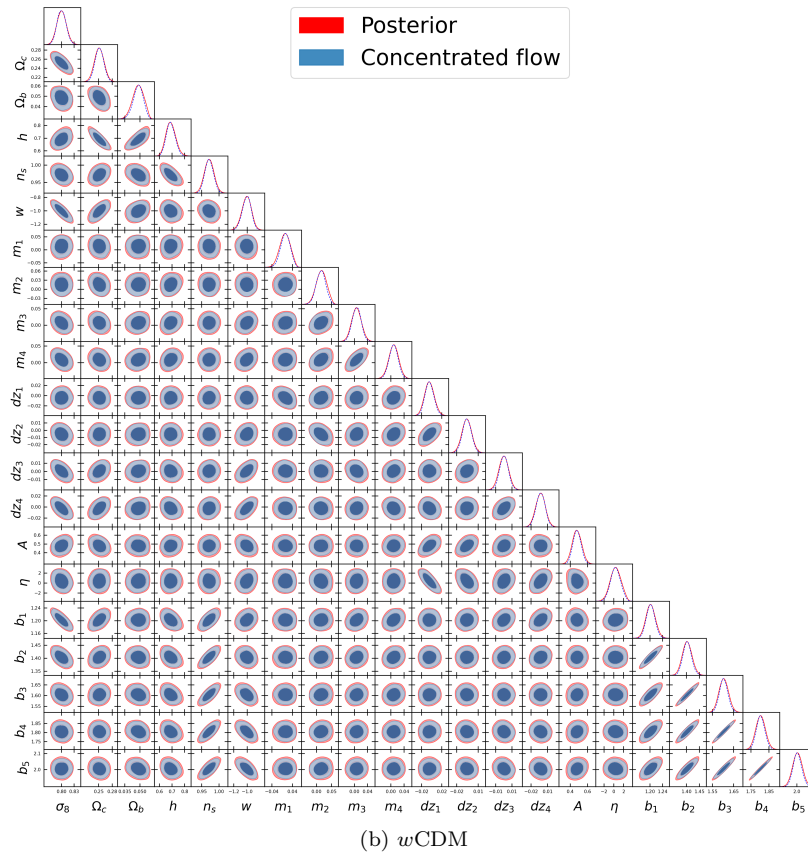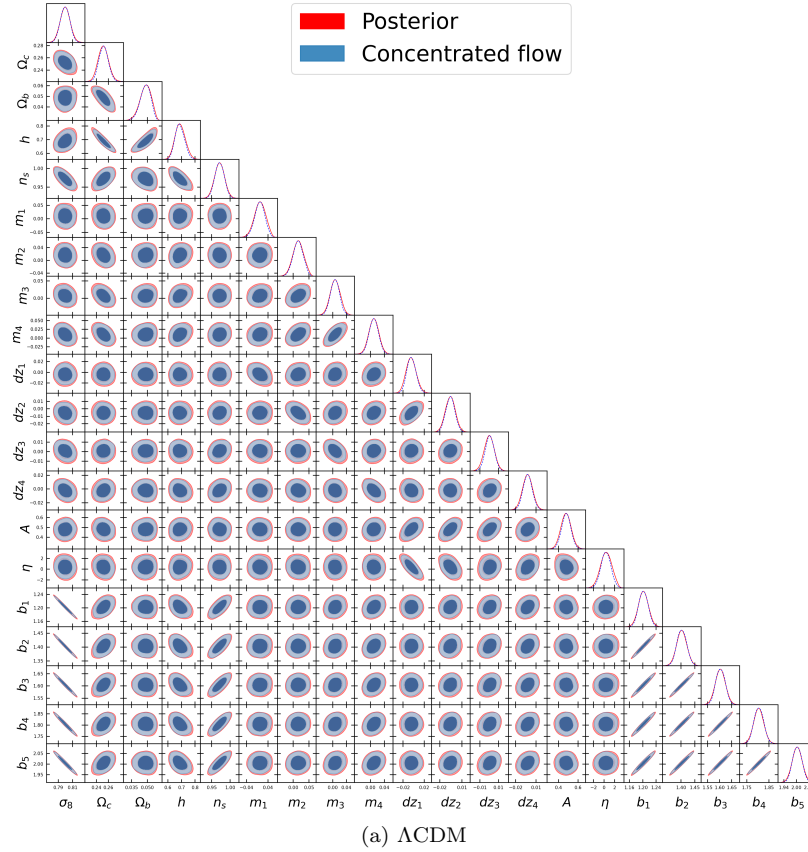
(a) ΛCDM

(b) wCDM

FIG. 8.— Corner plot of the sampled posterior (solid red) and rational quadratic spline flow trained on the posterior samples with temperature $T = 0.8$ (dashed blue) for the DES Y1 analysis example for (a) ΛCDM and (b) wCDM cosmological models. The internal importance target distribution given by the concentrated flow is contained within the posterior and has thinner tails, as required for the learned harmonic mean estimator, even in this higher dimensional case.

the `PolyChord` nested sampler ([Handley et al. 2015a,b](#)) in `Cobaya`, which provides a benchmark Bayesian evidence estimate. We perform the analysis twice, assuming either a ΛCDM or wCDM cosmological model, with the dark energy equation of state parameter w fixed to $w = -1$ or free to vary, respectively.

The ΛCDM and wCDM models have 20 and 21 parameters respectively. With the Metropolis-Hastings sampler, we run 64 chains per model, obtaining an average of approximately $5,800$ and $6,500$ samples per chain for ΛCDM and wCDM respectively. We discard 500 samples for burn-in in both cases. We train a rational quadratic flow consisting of 3 layers, with 128 spline bins, applying standardization, on half of the chains, and use the other half for inference.

Figure [8](#) shows the corner plots of the training samples alongside the flow at $T = 0.8$. It can be seen the flow also behaves as expected in this higher-dimensional practical setting, capturing the posterior distribution while being contained within it. Log evidence values, Bayes factors and computation time are reported in Table [1](#) for the learned harmonic mean estimator, nested sampling with `PolyChord` and by the naïve flow estimate introduced in [Spurio Mancini et al. (2023)](#) and described in Section [3.2.6](#).

Note that the values computed by the learned harmonic mean and nested sampling are in close agreement, showing a slight preference for ΛCDM, matching the configuration of our simulated setup. The values computed by the naïve estimator are in approximate agreement but exhibit an error two orders or magnitude larger than the error of the learned harmonic mean (in higher dimensional examples to be reported in an ongoing work we observe the naïve estimator failing much more catastrophically).

In terms of computational speed (summarized in Table [1](#) but reported in great detail here), sampling with `Cobaya` using the Metropolis-Hastings algorithm takes approximately 8 hours for ΛCDM and wCDM each on 64 CPU cores. The compute time added by `harmonic` is around 5 minutes on 1 GPU for training and 3 minutes on 128 CPU cores to estimate the evidence for each model. Using `PolyChord` takes approximately 47 hours for ΛCDM and wCDM each, on the same 64 CPU cores used for the Metropolis-Hastings sampling. The Metropolis-Hastings algorithm in this case is much quicker due to the use of a proposal covariance matrix based on a Planck cosmology ([Campagne et al. 2023](#)). Thanks to the flexibility of the learned harmonic estimator, we can leverage this advantage and choose Metropolis-Hastings over nested sampling, while still being able to estimate the Bayesian evidence and perform model comparison. Even in this higher dimensional setting, the learned harmonic mean only adds a few minutes of compute time on top of the sampler. This demonstrates the potential scalability of the method and its potential for computing the evidence from existing saved down MCMC chains.

5. CONCLUSIONS

In this work we outlined the learned harmonic mean estimator with normalizing flows, a robust, flexible and scalable estimator of the Bayesian evidence. Normalizing flows meet the core requirements of the learned impor-

tance target distribution of the learned harmonic mean estimator: namely, they provide a normalized probability distribution for which one can evaluate probability densities. We use them to introduce an elegant way to ensure the probability mass of the learned distribution is contained within the posterior, a critical requirement of the learned harmonic mean. This avoids the need for a bespoke training approach, resulting in a more robust and flexible estimator. Furthermore, flows offer the potential of greater scalability than the classical machine learning models considered previously.

To validate its accuracy, we applied the learned harmonic mean to several benchmark problems. Our method produced accurate results, even in cases where the original harmonic mean had been shown to fail. We also applied the learned harmonic mean to a practical cosmological example, the Dark Energy Survey Year 1 (DES Y1) data 3x2pt analysis. Even in this higher dimensional context for up to 21 parameters our method computed an estimate that was in excellent agreement with the conventional approach using nested sampling. This shows the potential for scalability of our method. Many existing methods of estimating the Bayesian evidence, including previous work on the learned harmonic mean, require careful parameter fine-tuning. Beyond the flow architecture, we only introduced one hyperparameter – the concentrated flow temperature T, which does not require any fine-tuning. We showed this empirically by considering a selected benchmark problem for a range of T values. The estimate remained accurate, demonstrating the robustness of our method.

Since the learned harmonic mean estimator is decoupled from the sampling method, it can be used in a wide variety of settings. This includes approaches such as simulation-based inference, variational inference and various MCMC methods where the evidence could not otherwise be computed accurately, such as the No U-Turn Sampler (NUTS) ([Hoffman & Gelman 2011](#)). When using MCMC methods for parameter estimation, the Bayesian evidence can be obtained essentially "for free" or even post-hoc from saved down MCMC chains. Since the estimator is agnostic to the sampling strategy, it is highly flexible. The best suited sampling strategy may be used for the problem at hand, as we demonstrated in the DES Y1 example, where Metropolis-Hastings accurately sampled the posterior much faster than nested sampling. In ongoing work we leverage the flexibility of the learned harmonic mean to demonstrate its use with NUTS and the CosmoPower-JAX emulator ([Spurio Mancini et al. 2022](#); [Piras & Spurio Mancini 2023](#)) to scale evidence calculation to ~ 150 dimensions. Overall, the learned harmonic mean estimator with normalizing flows is a robust, flexible and scalable tool for Bayesian model comparison that can be used in a variety of contexts.

REFERENCES

Abbott T., et al., 2018a, Physical Review D, 98
Abbott T. M., et al., 2018b, Physical Review D, 98, 043526
Aghanim N., et al., 2020, Astronomy & Astrophysics, 641, A6
Ashton G., et al., 2022, Nature Reviews Methods Primers, 2, 39
Bernardo J., Smith A., 1994, Wiley Online Library
Bradbury J., et al., 2018, JAX: composable transformations of Python+NumPy programs, http://github.com/google/jax
Brewer B. J., Pártay L. B., Csányi G., 2011, Statistics and Computing, 21, 649
Brout D., et al., 2022, The Astrophysical Journal, 938, 110
Buchner J., 2021, Journal of Open Source Software, 6, 3001
Cai X., McEwen J. D., Pereyra M., 2022, Statistics and Computing, 32
Campagne J.-E., et al., 2023, The Open Journal of Astrophysics, 6
Carron J., Mirmelstein M., Lewis A., 2022, Journal of Cosmology and Astroparticle Physics, 2022, 039
Chib S., 1995, Journal of the American Statistical Association, 90, 1313
Clyde M., Berger J., Bullard F., Ford E., Jefferys W., Luo R., Paulo R., Loredo T., 2007, in Statistical challenges in modern astronomy IV. p. 224
DES Collaboration et al., 2024, The Dark Energy Survey: Cosmology Results With 1500 New High-redshift Type Ia Supernovae Using The Full 5-year Dataset (arXiv:2401.02929)
DESI Collaboration et al., 2016, The DESI Experiment Part I: Science,Targeting, and Survey Design (arXiv:1611.00036)
DeepMind et al., 2020, The DeepMind JAX Ecosystem, http://github.com/deepmind
Dillon J. V., et al., 2017, TensorFlow Distributions (arXiv:1711.10604)
Dinh L., Sohl-Dickstein J., Bengio S., 2017, in International Conference on Learning Representations. https://openreview.net/forum?id=HkpbnH9lx
Dozat T., 2016, in Proceedings of the 4th International Conference on Learning Representations. pp 1–4
Durkan C., Bekasov A., Murray I., Papamakarios G., 2019, Advances in neural information processing systems, 32
Feroz F., Hobson M. P., 2008, Monthly Notices of the Royal Astronomical Society, 384, 449–463
Feroz F., Hobson M. P., Bridges M., 2009a, MNRAS, 398, 1601
Feroz F., Hobson M. P., Bridges M., 2009b, Monthly Notices of the Royal Astronomical Society, 398, 1601–1614
Feroz F., Hobson M. P., Cameron E., Pettitt A. N., 2019, The Open Journal of Astrophysics, 2
Foreman-Mackey D., Hogg D. W., Lang D., Goodman J., 2013, PASP, 125, 306
Friel N., Wyse J., 2012, Statistica Neerlandica, 66, 288
Gelfand A. E., Dey D. K., 1994, Journal of the Royal Statistical Society: Series B (Methodological), 56, 501
Green P. J., 1995, Biometrika, 82, 711
Handley W. J., Hobson M. P., Lasenby A. N., 2015a, Monthly Notices of the Royal Astronomical Society: Letters, 450, L61–L65
Handley W. J., Hobson M. P., Lasenby A. N., 2015b, Monthly Notices of the Royal Astronomical Society, 453, 4385–4399
Hastings W. K., 1970, Biometrika, 57, 97
Heek J., Levskaya A., Oliver A., Ritter M., Rondepierre B., Steiner A., van Zee M., 2023, Flax: A neural network library and ecosystem for JAX, http://github.com/google/flax

Hoffman M. D., Gelman A., 2011, The No-U-Turn Sampler: Adaptively Setting Path Lengths in Hamiltonian Monte Carlo (arXiv:1111.4246)
Joachimi B., Bridle S. L., 2010, A&A, 523, A1
Kingma D. P., Ba J., 2017, Adam: A Method for Stochastic Optimization (arXiv:1412.6980)
Lenk P., 2009, Journal of Computational and Graphical Statistics, 18, 941
Madhavacheril M. S., et al., 2024, The Astrophysical Journal, 962, 113
McEwen J. D., Wallis C. G. R., Price M. A., Mancini A. S., 2021, Machine learning assisted Bayesian model comparison: learnt harmonic mean estimator (arXiv:2111.12720)
Metropolis N., Rosenbluth A. W., Rosenbluth M. N., Teller A. H., Teller E., 1953, J. Chemical Physics, 21, 1087
Murphy K. P., 2022, Probabilistic Machine Learning: An introduction. MIT Press, probml.ai
Neal R. M., 1994, JR Stat Soc Ser A (Methodological), 56, 41
Newton M. A., Raftery A. E., 1994, Journal of the Royal Statistical Society: Series B (Methodological), 56, 3
Papamakarios G., Nalisnick E., Rezende D. J., Mohamed S., Lakshminarayanan B., 2021, The Journal of Machine Learning Research, 22, 2617
Piras D., Spurio Mancini A., 2023, The Open Journal of Astrophysics, 6
Polanska A., Price M. A., Spurio Mancini A., McEwen J. D., 2023, Physical Sciences Forum, 9
Raftery A. E., Newton M. A., Satagopan J. M., Krivitsky P. N., 2006, Preprint
Robert C. P., Wraith D., 2009, in Aip conference proceedings. pp 251–262
Rubin D., et al., 2023, Union Through UNITY: Cosmology with 2,000 SNe Using a Unified Bayesian Framework (arXiv:2311.12098)
Skilling J., 2006, Bayesian Analysis, 1, 833
Smith J. W., Everhart J. E., Dickson W., Knowler W. C., Johannes R. S., 1988, in Proceedings of the annual symposium on computer application in medical care. p. 261
Speagle J. S., 2020, MNRAS, 493, 3132
Spurio Mancini A., Piras D., Alsing J., Joachimi B., Hobson M. P., 2022, Monthly Notices of the Royal Astronomical Society, 511, 1771
Spurio Mancini A., Docherty M. M., Price M. A., McEwen J. D., 2023, RAS Techniques and Instruments, 2, 710–722
Srinivasan R., Crisostomi M., Trotta R., Barausse E., Breschi M., 2024, floZ: Evidence estimation from posterior samples with normalizing flows (arXiv:2404.12294)
Torrado J., Lewis A., 2019, Astrophysics Source Code Library, pp ascl–1910
Trotta R., 2008, Contemporary Physics, 49, 71
Williams E. J., 1959, Regression analysis. Wiley, New York
Williams M. J., Veitch J., Messenger C., 2021, Physical Review D, 103
van Haasteren R., 2014, in , Gravitational Wave Detection and Data Analysis for Pulsar Timing Arrays. Springer, pp 99–120

This paper was built using the Open Journal of Astrophysics LATEX template. The OJA is a journal which provides fast and easy peer review for new papers in the astro-ph section of the arXiv, making the reviewing process simpler for authors and referees alike. Learn more at http://astro.theoj.org.